Effects of organic additives on microstructure and mechanical properties of porous Si$_3$N$_4$ ceramics

YU FANGLI, WANG HUANRUI, YANG JIANFENG* and GAO JIQIANG

State Key Laboratory for Mechanical Behaviour of Materials, Xi'an Jiaotong University, Xi'an 710049, P.R. China

Abstract.   Green bodies of porous Si$_3$N$_4$ ceramics were shaped by extrusion technique using different organic additives as binder during extrusion molding. Different porosity, microstructures and mechanical properties after the extrusion, drying, debinding and sintering stages were investigated. The solid slurry content of 70–75% and extrusion pressure of 0·5–1·0 MPa had played a decisive role in the smooth realization of extrusion molding. The porous Si$_3$N$_4$ ceramics were obtained with excellent properties using 4% hydroxypropyl methyl cellulose (HPMC) as binder and polyethylene glycol (PEG) of molecular weight, 1000, as plasticizer with a density of 1·91 g cm^{-3}, porosity of 41·70%, three-point bending strength of 166·53 ± 20 MPa, fracture toughness of 2·45 ± 0·2 MPa m$^{1/2}$ and Weibull modulus (m) of 20·75.

Keywords.   Organic additives; processing; microstructure; mechanical properties; porous Si$_3$N$_4$ ceramics; Weibull distribution.

1.   Introduction

Porous Si$_3$N$_4$ ceramics is a prominent filtering material due to its excellent mechanical, high-temperature thermal and chemical stability (Kawaia and Yamakawa 1997; Shigegaki *et al* 1997). Porous Si$_3$N$_4$ ceramics with high porosity are of interest for engineering applications, as gas filters, separation membranes, and catalyst supports at high temperature (Haslam *et al* 2000; Oh *et al* 2000; Corbin *et al* 2001). Many studies have been devoted into the molding methods of porous Si$_3$N$_4$ ceramics, such as compression molding, injection molding, isostatic pressing, slip casting and extrusion. Also it is clear that people have paid more attention to extrusion recently, actually, extrusion, a shaping technique mainly used to produce ceramic items with a constant cross-sectional area, can be used to replace the current shaping methods in some fields because of its high throughput and ability to fabricate complex products (Raupp-Pereira *et al* 2007; Kaya and Butler 2002; Isobe *et al* 2006, 2007). Furthermore, the manufacturing cost of porous Si$_3$N$_4$ ceramics can be lowered substantially by extrusion, thus making their widespread industrial applications possible. In extrusion process, selection of binder plays a crucial part in preparing extrusive plastic paste. It is reported that several groups of organic additives have been used as binder in extrusion of ceramics (Treischel and Emrich 1946). However, a few papers about the effect of organic additives on microstructure and mechanical properties of porous Si$_3$N$_4$

ceramics were presented with an in-depth discussion. On the other hand, the binder usually is removed thermally from green body before sintering, so it means that organic additives also can be utilized as a pore former in a certain extent.

In the present study, green bodies of porous Si$_3$N$_4$ ceramics were shaped by extrusion technique using different organic additives such as carboxymethyl cellulose (CMC, viscosity, 800~1200), methyl cellulose (MC), and hydroxypropyl methyl cellulose (HPMC) as binder. Different microstructures and mechanical properties after the extrusion, drying, debinding and sintering stages were investigated and the feasibility of using organic additives as extrusion additives to prepare porous Si$_3$N$_4$ ceramics was evaluated in detail.

2.   Experimental

2.1   *Preparation of samples*

Commercially available Si$_3$N$_4$ powder (Shanghai Junyu Co. Ltd., Shanghai, China; α-Si$_3$N$_4$ ratio: > 95%, mean particle size: 1·2 μm, main impurities by weight: O = 1·6%; C < 0·2%; Cl, Fe, Ca, and Al$_2$O$_3$ < 80 ppm) was selected for use in this study. Y$_2$O$_3$ and Lu$_2$O$_3$ were used as sintering additives, CMC, MC, and HPMC as binder, and polyethylene glycol (PEG) as plasticizer. Castor oil was selected as lubricant to reduce the friction force between Si$_3$N$_4$ particles, and glycerol as moisturizing agent.

Figure 1 shows a flow diagram for fabricating porous silicon nitride ceramics. 5 wt.% Y$_2$O$_3$ or Lu$_2$O$_3$ and

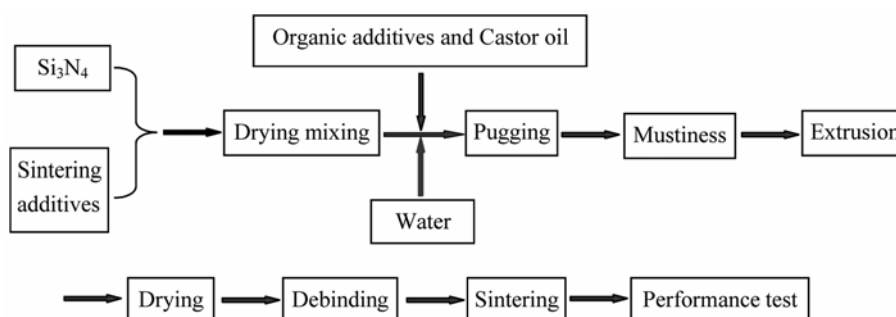*Author for correspondence (yang155@mail.xjtu.edu.cn)

Figure 1. Flow diagram for fabricating porous silicon nitride samples.

α-Si$_3$N$_4$ powders were firstly dry mixed in a planetary mixer for 2·5 h. Pro rata organic additives, castor oil and water were added into the dry mixture. The obtained mixture was then kneaded in an alumina mortar with a pestle for 20 min, providing a high-shear mixing to break up agglomerates and obtain homogeneous paste. Then the resulting paste was decayed for 12 h and extruded to form the rods, 8·8 mm in diameter, through a homemade piston-type extruder (barrel diameter: 25 mm, length of die land: 12 mm, entrance angle of conical die: 31·8°) at room temperature. The extrusion force was exerted by a table-top testing machine (Instron 1195, Instron Co., Buckinghamshire, England), which allowed the extrusion force to be recorded as a function of piston displacement. The moving velocity of piston was 20 mm/min. The testing machine also was used to measure three-point bending strength below. The extruded rods were subsequently cut into about 40 mm length. The cut green rods were firstly dried at 40°C for 10 h to remove moisture. The dried rods were subsequently thermally sintered at 650°C with a heating rate of 30°C/h to remove organic additives and lubricant. Finally, the samples were put into a BN-coated graphite crucible and sintered in a graphite resistance furnace (High multi-5000, Fijidempa Co. Ltd., Osaka, Japan) at 1800°C under 0·525 MPa nitrogen (99·999%) atmosphere for 2 h with a heating rate of 15°C/min, no powder bed was covered on the samples during sintering.

2.2 *Examination of properties*

Bulk density of the samples after extrusion was determined by measuring the dimensions and weight, and porosity was calculated from the bulk density and theoretical density, which was calculated by the rule of mixtures. The bulk density and open porosity of the samples after other stages were measured by the Archimedes displacement method using distilled water.

The samples after sintering were machined into test bars of $30 \times 4 \times 3$ mm^3 for bending strength measurement. All surfaces of the sintered test bars were finally ground on an 800-grit diamond wheel, and the edges were tilted. The directions of both the diamond grinding and tilting were parallel to that of the bar length. All three-point bending strengths were measured with a span of 16 mm at a cross-head speed of 0·5 mm/min, using Instron universal testing machine. Fracture toughness was determined by a single-edge precracked beam (SEPB). The precracked specimens were tested at a stroke rate of 0·05 mm/min using a three-point bending fixture with a span of 16 mm using the same testing machine as the bending strength test.

Crystalline phases were identified by X-ray diffraction (XRD) (D/MAX-2400X, Rigaku Co. Ltd., Tokyo, Japan) analysis using CuK$_\alpha$ radiation. The microstructures were characterized by scanning electron microscope (SEM, S-2700, Hitachi, Japan). The fracture surfaces after the bending test and the polished surfaces, coated with gold, were used for SEM observation, respectively.
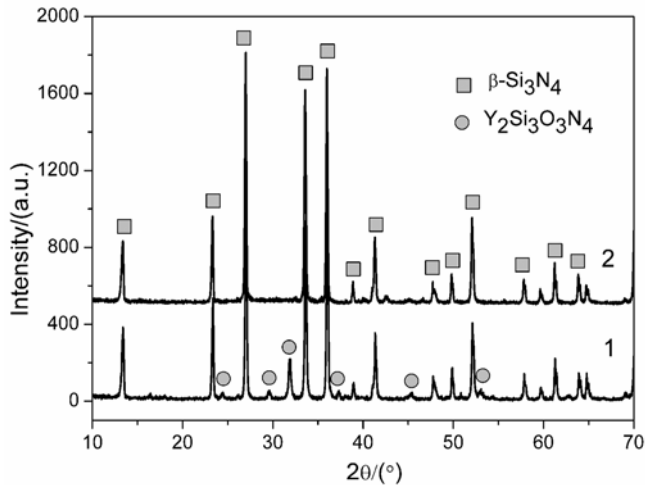
3. Results and discussion

3.1 *Effect of CMC as binder*

The solution concentration for CMC as binder was 2·5%, 15% PEG of molecular weight 10000 as plasticizer. The compositions of the test samples with 5 wt.% Y$_2$O$_3$ and Lu$_2$O$_3$ are listed in table 1. The most stable and suitable slurry was obtained from a solid slurry content of 65~80%, when the slurry was too diluted, it was not easy to form, and too dried, it was difficult to extrude, so the solid slurry content of 70~75% and extrusion pressure of 0·5~1·0 MPa were chosen in the experiment.

Figure 2 shows XRD patterns of samples 1 and 2, the main phase was β-Si$_3$N$_4$, without α-Si$_3$N$_4$ phase detected, and confirming a full transformation from α-Si$_3$N$_4$ to β-Si$_3$N$_4$ during sintering by a solution-precipitation process. The acicular microstructure was believed that it was a result of the anisotropic growth of the hexagonal Si$_3$N$_4$ grains to maximize the area of the low energy (100) prismatic planes. The newly formed β-Si$_3$N$_4$ phase had an elongated hexagonal rod morphology, which formed an interlocking microstructure and was considered responsible for the superior mechanical properties of Si$_3$N$_4$ ceramics (Lper 1995). No second phase particles were identified in

Table 1. Compositions of the test samples with 5 wt% Y_2O_3 and Lu_2O_3.

Samples	Composition in mass	PEG (%)	CMC (%)	Castor oil (%)
1	5% Y_2O_3 + 95% Si_3N_4	35	20	8
2	5% Lu_2O_3 + 95% Si_3N_4	35	20	8

Figure 2. XRD patterns of samples 1 and 2.

sample 2, indicating that Lu_2O_3 were dissolved in the eutectic liquid during the sintering process. However, a small amount of $Y_2Si_3O_3N_4$ exists in sample 1, formed by the reaction between Y_2O_3, Si_3N_4 and SiO_2.

SEM micrographs of fracture surfaces of the sintered samples with different sintering additives are given in figure 3. It was obvious that these samples showed a typical bimodal microstructure composed of large elongated β-Si_3N_4 grains and small β-Si_3N_4 matrix grains. Compared with samples 1 and 2, it was striking that sample 2 had a small amount of larger elongated β-Si_3N_4 grains and a finer, higher aspect ratio of β-Si_3N_4 matrix grains. The microstructure of the porous Si_3N_4 ceramics added with Lu_2O_3 was better than those added with Y_2O_3, the explanation for the microstructural formation for the different ceramics with different types of oxides had been well documented (Yang *et al* 2006; Yu *et al* 2008).

Figure 4 shows the density, porosity and three-point bending strength (flexural strength) of the porous Si_3N_4 ceramics. The porous Si_3N_4 ceramics with three-point bending strengths of 42·18 ± 12 and 57·63 ± 15 MPa and porosities of 45·56% and 47·32%, respectively were obtained. The resultant porous Si_3N_4 ceramics exhibited much lower strength in comparison with other porous Si_3N_4 ceramics (Yang *et al* 2000, 2002, 2003a). The explanations are given as follows. The molecular structural formulas of CMC and PEG are shown in figure 5. CMC acted as a binder and effective deflocculant simul-

taneously because of the polar groups such as $-CH_2OCH_2COONa$ and $-OH$, adding CMC conferred to the suspensions a shear thinning behaviour, especially in the lower shear rate range, followed by a trend to a Newtonian fluid behaviour. This flow behaviour was typical of well dispersed and highly concentrated suspensions (Tari 1998a, b). So CMC was very good for use in slip casting molding, but went against extrusion molding. The defects were more easily generated in molding process because of low viscosity of the slurries, so the prepared porous Si_3N_4 ceramics had lower flexural strength. And adding 15% PEG of molecular weight, 10000, as plasticizer, the molecular chain rigidities tended to increase with increasing molecular weight, which induced extrusion molding with difficulty. Even if the green body was formed, the molding samples were more easily to produce a great number of micro cracks because of release of residual stress produced in resisting molecular chain deformability in drying, debinding and sintering, the resultant porous Si_3N_4 ceramics showed worse mechanical properties due to a great number of micro cracks. So the PEG of molecular weight, 10000, was not suitable for plasticizer, and PEG of molecular weight, 1000, was chosen in the next experiment.

3.2 *Effect of MC and HPMC as binder*

2%, 4% MC and 4% HPMC were selected as binder and 15% PEG of molecular weight, 1000, as plasticizer. The compositions of the test samples with different concentrations of MC and HPMC are listed in table 2.

Table 3 shows mechanical properties of the porous Si_3N_4 ceramics. The results showed that the mechanical properties of the sintering sample with compositions of 4% MC + 1000 PEG and 4% HPMC + 1000 PEG, and a solid slurry content of 75% showed very excellent mechanical properties in comparison with other compositions. Although the green density of the sample with composition of 2% MC + 1000 PEG was lower, the density of porous Si_3N_4 ceramics was similar to the other compositions due to the shrinking in the sintering process, which was very detrimental for mechanical properties.

For analysing three-point bending strength distribution of the ceramics material, Weibull (1951) proposed a two-parameter distribution function to characterize the strength of brittle materials. More clearly, a low *m* value indicates non-uniform distribution of highly variable
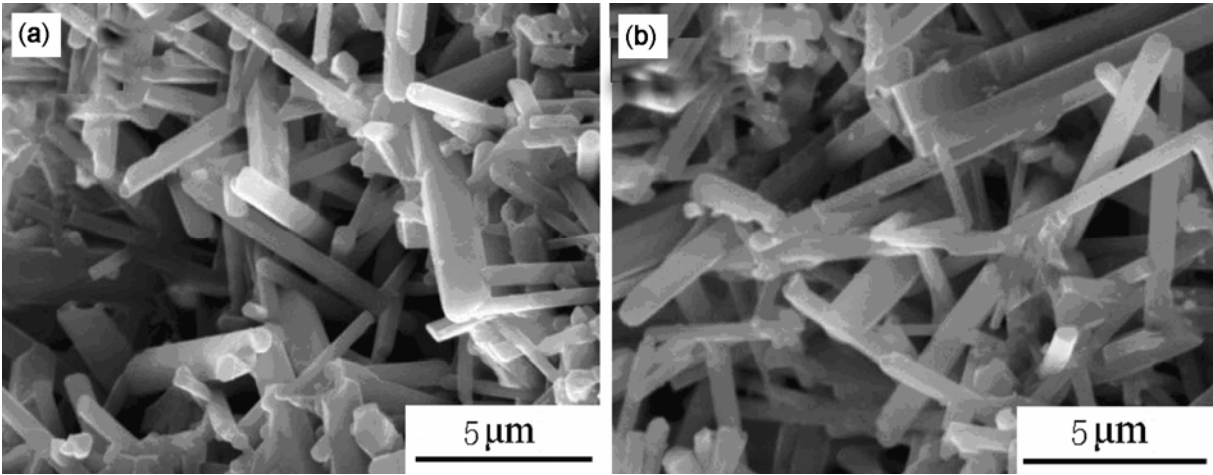
Figure 3. SEM micrographs of (**a**) sample 1 and (**b**) sample 2.

Table 2. Compositions of the test samples with different concentrations of MC and HPMC.

Compositions (wt.%)	Binder (%)	PEG (%)	Castor oil (%)
5% Lu_2O_3 + 95% Si_3N_4 + 2% MC (concentration)	25	5	4
5% Lu_2O_3 + 95% Si_3N_4 + 4% MC (concentration)	25	5	4
5% Lu_2O_3 + 95% Si_3N_4 + 4% HPMC (concentration)	25	5	4

Figure 4. Density, porosity and three-point bending strength (flexural strength) of porous Si_3N_4 ceramics.
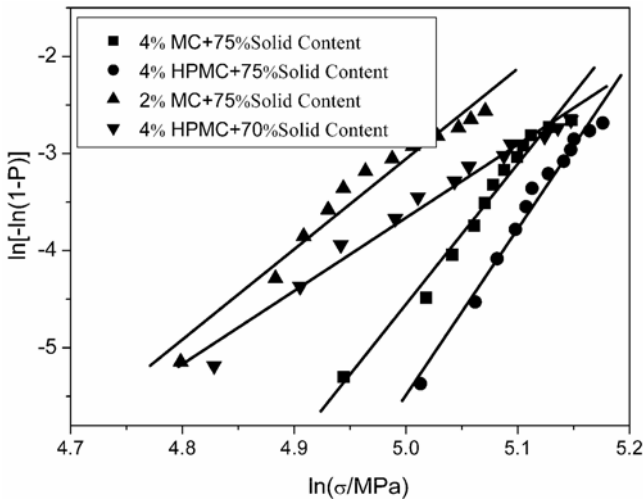

Figure 6. Weibull statistics analysis results of the samples adding different binder and solid slurry contents.
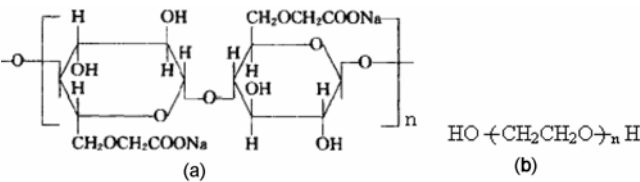

Figure 5. Molecular structural formula of (**a**) CMC and (**b**) PEG.

crack length (broad strength distribution), while a high *m* value implicates uniform distribution of highly homogeneous flaws with narrower strength distribution. Typically, for structural ceramics, *m* varies between 5 and 30, depending on the processing conditions (Bazant 2004; Zeng *et al* 2006), so the Weibull distribution function is widely used to characterize the fracture strength of the porous Si_3N_4 ceramics. Figure 6 shows Weibull statistics analysis where failure probability was plotted versus
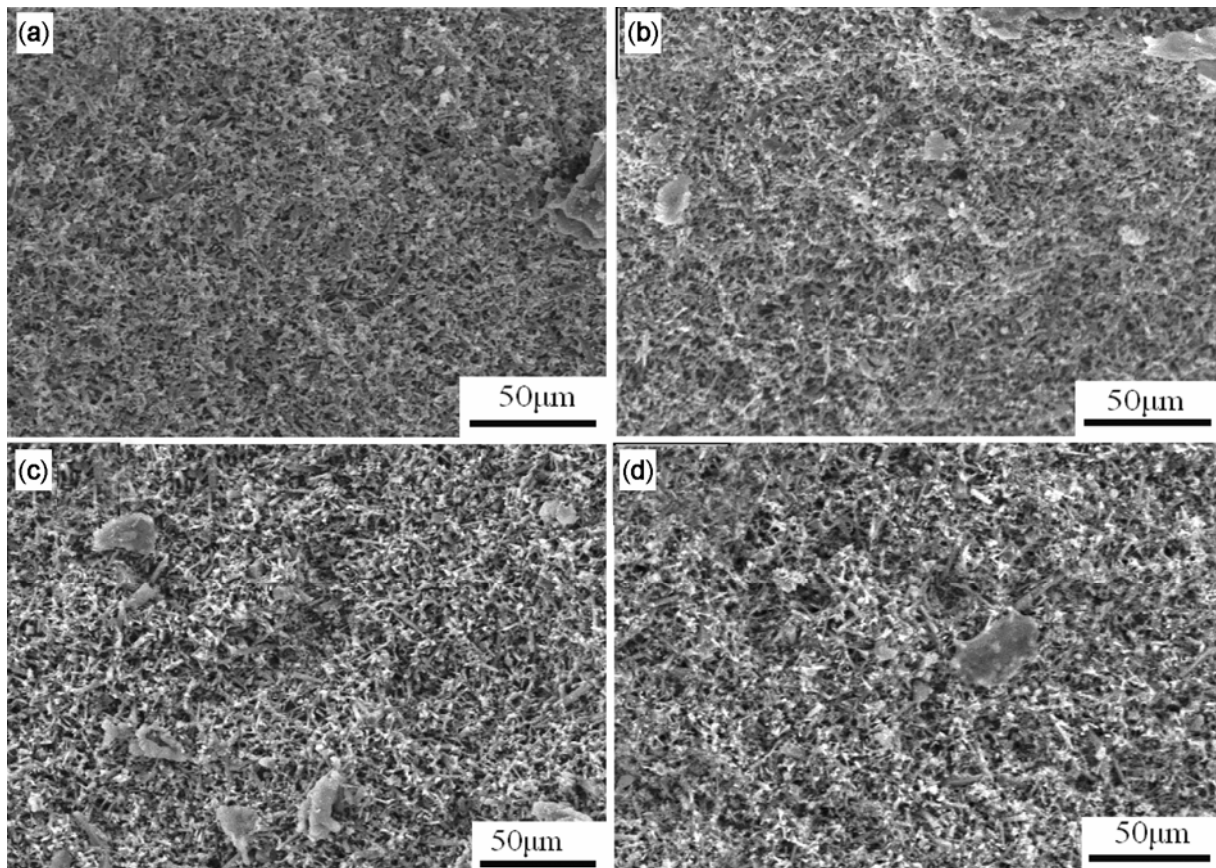
Figure 7. SEM micrographs of porous Si₃N₄ ceramics with different concentrations of binder and solid slurry contents. (**a**) 4% HPMC + solid slurry content 75%; (**b**) 4% MC + solid slurry content 75%; (**c**) 2% MC + solid slurry content 75% and (**d**) 4% HPMC + solid slurry content 70%.
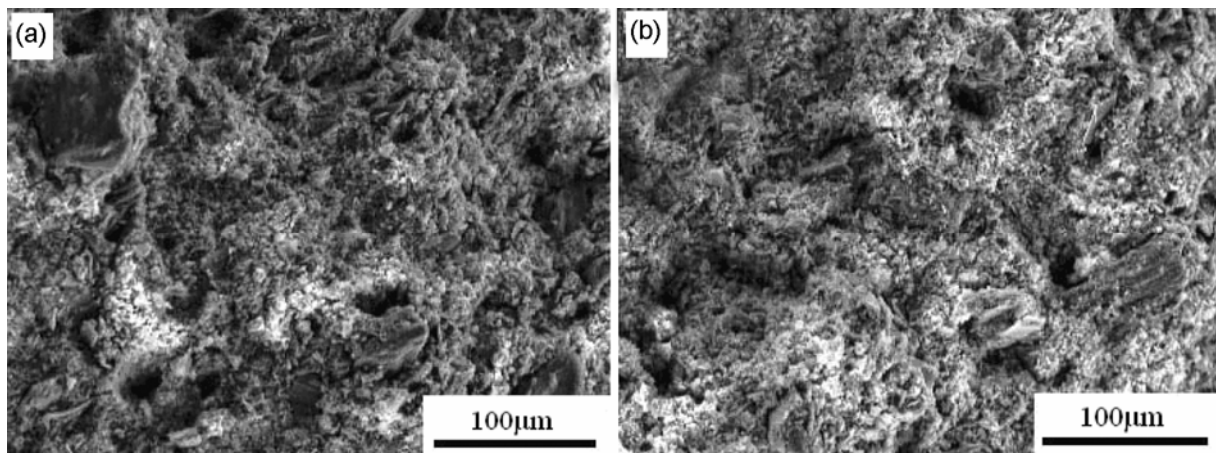

Figure 8. SEM micrographs of the green body after sintering with compositions of (**a**) 4% MC and (**b**) 4% HPMC.

applied load. All the strength data are tabulated in table 4. For sample with compositions of 4% MC + 1000 PEG and 4% HPMC + 1000 PEG and a solid slurry content of 75%, the Weibull modulus (m) was very high, which indicated uniform distribution of highly homogeneous flaws with narrower strength distribution.
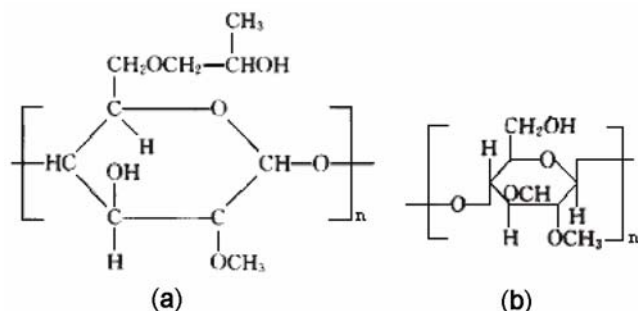
Figure 7 gave SEM micrographs of fracture surfaces of the sintered samples with different solid slurry contents and binder. It was obvious that the samples showed a typical bimodal microstructure composed of large elongated β-Si₃N₄ grains and small β-Si₃N₄ matrix grains. The microstructure of the porous Si₃N₄ ceramics added

Table 3. Mechanical properties of the porous Si_3N_4 ceramics.

Solid slurry content (%)	75%		70%	
Compositions	2% MC + PEG	4% MC + PEG	4% HPMC + PEG	4% HPMC + PEG
Green density (g·cm^{-3})	1·66	1·69	1·71	1·70
Green porosity (%)	37·36	35·39	35·62	36·43
Density (g·cm^{-3})	1·86	1·85	1·91	1·95
Porosity (%)	42·92	43·08	41·70	40·29
σ_b (MPa)	141·02 ± 22	160·35 ± 24	166·53 ± 20	152·70 ± 25
K_{IC}/(MPa·m$^{1/2}$)	2·21 ± 0·3	2·39 ± 0·2	2·45 ± 0·2	2·34 ± 0·1

Table 4. Weibull modulus (m) of the samples with different binder and solid slurry contents.

Solid slurry content (%)	Compositions (wt.%)	Weibull modulus (m)
75	2% MC + PEG	15·84
	4% MC + PEG	18·38
	4% HPMC + PEG	20·75
70	4% HPMC + PEG	13·42

Figure 9. Molecular structural formula of (**a**) HPMC and (**b**) MC.

with compositions of 4% HPMC + 1000 PEG and 4% MC + 1000 PEG and a solid slurry content of 75% were better than those added with compositions of 2% MC, and a solid slurry content of 70%. It was reasonably believed that the concentration of binders and solid slurry content had great effect on properties of porous Si_3N_4 ceramics.

Figure 8 showed SEM micrographs of samples after debinding. Compared with two micrographs, the micrograph with 4% HPMC was more uniform than that of 4% MC. Figure 9 showed the molecular structural formula of MC and HPMC. The hydroxyl in the molecular structural formula of MC was close to the molecular ring, and the hydroxyl in the molecular structural formula of HPMC was connected with long molecular groups, so molecular polarity of HPMC was more stronger than MC, HPMC was easier to adsorb moisture and keep humidity, which had a good performance in the drying and debinding process, and not easier to deform and crack.

4. Conclusions

Green bodies of porous Si_3N_4 ceramics were shaped by extrusion technique using CMC, MC and HPMC as binder in subsequent process stages. The solid slurry content of 70~75% and extrusion pressure of 0·5~1·0 MPa had played a decisive role in the smooth realization of extrusion molding. The resultant porous Si_3N_4 ceramics with high porosity, well-developed microstructures, and outstanding mechanical properties were obtained. Using 15% PEG of molecular weight, 1000, as plasticizer, castor oil as lubricant and glycerol as moisturizing agent, 4% MC and HPMC were most suitable for extrusion molding. The porous Si_3N_4 ceramics were obtained with excellent properties using 4% HPMC as binder, the density of 1·91 g·cm^{-3}, porosity of 41·70%, and three-point bending strength of 166·53 ± 20 MPa, toughness fracture of 2·45 ± 0·2 MPa·m$^{1/2}$ and Weibull modulus of 20·75.

Acknowledgements

References

Bazant Z P 2004 *Prob. Eng. Mech.* **19** 307
Corbin S F, Lee J and Qiao X 2001 *J. Am. Ceram. Soc.* **84** 41
Haslam J J, Beroth K E and Lange F F 2000 *J. Eur. Ceram. Soc.* **20** 607
Isobe T, Tomita T, Kameshima Y, Nakajima A and Okada K 2006 *J. Eur. Ceram. Soc.* **26** 957
Isobe T, Kameshima Y, Nakajima A and Okada K 2007 *J. Eur. Ceram. Soc.* **27** 61
Kawai C and Yamakawa A 1997 *J. Am. Ceram. Soc.* **80** 2705
Kaya C and Butler E G 2002 *J. Eur. Ceram. Soc.* **22** 1917
Lper A M 1995 *Phase diagrams on advanced ceramics: chemical and metallurgical products II [C]* (ed.) Y T Tseng (PA: Towanda) pp 127–128
Oh S T, Tajima K I, Ando M and Ohji T 2000 *J. Am. Ceram. Soc.* **83** 1314

Raupp-Pereira F, Ribeiro M J, Segadaes A M and Labrincha J A 2007 *J. Eur. Ceram. Soc.* **27** 2333

Shigegaki Y, Brito M E, Hirao K, Toriyama M and Kanzaki S 1997 *J. Am. Ceram. Soc.* **80** 495

Tarì G, Ferreira J M F and Lyckfeldt O 1998a *J. Eur. Ceram. Soc.* **18** 386

Tarì G, Fonseca A T and Ferreira J M F 1998b *Br. Ceram. Trans.* **97** 259

Treischel C C and Emrich E W 1946 *J. Am. Ceram. Soc.* **29** 129

Weibull W 1951 *J. Appl. Mech.* **18** 293

Yang J, Yang J F, Shan S Y and Gao J Q 2006 *J. Am. Ceram. Soc.* **89** 3843

Yang J F, Ohji T and Niihara K 2000 *J. Am. Ceram. Soc.* **83** 2094

Yang J F, Ohji T, Kanzaki S, Díaz A and Hampshire S 2002 *J. Am. Ceram. Soc.* **85** 1512

Yang J F, Deng Z Y and Ohji T 2003a *J. Eur. Ceram. Soc.* **23** 371

Yang J F, Zeng Y P, Ohji T, Kanzaki S and Zhang G J 2003b *J. Ceram. Soc. Jpn* **111** 758

Yu F L, Yang J F, Xue Y H, Gao J Q and Jin Z H 2008 *J. Chin. Ceram. Soc.* **36** 1037

Zeng L K, Wang H and Luo M H 2006 *Preparation and application of porous functional ceramics* (Beijing: Chemical Industry Publishers) p. 95